CHAPTER-1

Introduction

1.1 Thesis Abstract

The importance of gas sensing technologies has grown significantly due to their role in monitoring environmental contaminants and maintaining safety across a range of applications. The present study investigates the advancement and utilization of gas sensors utilizing organic field-effect transistors (OFETs). Organic semiconductors possess distinct benefits, such as their inherent flexibility, cost-effectiveness in manufacturing, and the ability to customize their chemical sensing capabilities. The research starts by undertaking the design and manufacture of gas sensors based on organic field-effect transistors (OFETs), employing organic semiconductor materials. The sensing method is dependent on the change in the mobility of charge carriers inside the transistor channel, which occurs as a result of particular interactions with gases. The selection of organic materials is meticulously evaluated in order to optimize sensitivity and selectivity towards certain gases of interest. The primary objective of experimental research is to analyze and evaluate the sensor's reaction to various gases, encompassing volatile organic compounds (VOCs) as well as prevalent environmental contaminants. The sensors demonstrate exceptional performance for Hydrogen sulfide gas sensing in terms of their sensitivity, response time, and recovery properties. The investigation also includes the examination of the impact of environmental variables, such as temperature and humidity, on the functioning of sensors. Moreover, the study investigates the improvement of sensor characteristics, including channel and gate dielectric properties, in order to improve the overall performance of the sensor. The objective is to develop a gas sensing platform that is both dependable and replicable, making it ideal for practical use in real-world scenarios. The advantages of OFET-based sensors, such as their potential for downsizing and integration into flexible electronic devices, are underscored through a comparative study with existing gas sensing

technologies. In summary, this research makes a valuable contribution to the progressing domain of gas sensing by showcasing the viability and prospects of gas sensors based on organic field-effect transistors (OFETs). The results of this study offer valuable information on the enhancement of sensor performance and lay the foundation for the creation of innovative, adaptable, and affordable gas sensing platforms. These platforms have the potential to be utilized in several fields, such as environmental monitoring, industrial safety, and healthcare.

1.2 A Brief History and Overview of Gas Sensors

Gas sensors play a pivotal role in monitoring and detecting the presence of various gases in our environment, serving a wide range of applications from industrial processes to environmental safety [1][2]. These sensors are crucial for ensuring the well-being of both humans and the planet by providing early warnings about potential hazards and facilitating efficient control of processes. The evolution of gas sensors spans a fascinating journey, marked by advancements in technology, materials, and ongoing efforts to safeguard human lives and the environment from the potential dangers posed by hazardous gases. Here's a brief overview of key milestones in the history of gas detection:

Early 19th Century: The earliest forms of gas detection were rudimentary and often relied on human senses. Miners, for example, used canaries to detect the presence of toxic gases in coal mines. If the canary showed signs of distress, it signaled the presence of harmful gases like carbon monoxide.

Late 19th Century: The development of chemical indicators marked an early step in gas detection. These indicators, often paper strips impregnated with reactive substances, changed color in the presence of specific gases.

Early 20th Century: The introduction of flame safety lamps in coal mines provided a visual indication of the presence of flammable gases. These lamps were designed to prevent explosions by enclosing the flame within a mesh screen.

Modern era of gas detection: While the utilization of flame light represented a significant advancement in gas detection technology, it did not prove to be universally applicable across all sectors. Hence, the catalytic sensor may be considered as the initial gas detector that exhibits similarities to modern technologies. The inception of catalytic gas sensors may be traced back to the years 1926-1927 when Dr. Oliver Johnson pioneered the creation of the catalytic combustion sensor. Dr. Johnson, an employee of the Standard Oil Company in California (now known as Chevron), initiated research and development efforts aimed at devising a technique for detecting flammable mixtures present in the atmosphere. The primary objective of this endeavour was to mitigate the risk of explosions occurring within fuel storage tanks. The development of a demonstration model occurred in 1926, which was subsequently designated as Model A. Production of the inaugural "electric vapor indicator" meter commenced in 1927, coinciding with the introduction of the Model B. Johnson-Williams Instruments (J-W Instruments), established in 1928 in Palo Alto, California, by Dr. Oliver Johnson and Phil Williams, holds the distinction of being the inaugural gas detection firm worldwide. The catalytic sensors operate based on the fundamental idea that the oxidation of a gas results in the generation of thermal energy. The sensor operates by detecting changes in temperature that are directly proportional to the gas concentration. Although this represented progress in the advancement of gas detection technology, it initially necessitated manual operation for obtaining readings.

Consequently, researchers have continuously investigated and advanced numerous types of gas sensors. Within this context, six exemplary categories of gas sensors are presented: resistive, optical, electro-chemical, Surface acoustic wave (SAW), calorimetric, and field-effect transistor-type (FET-type) gas sensors.

Resistive gas sensors detect target gases by measuring the change in resistance of the sensor after exposure to gases [3]. The sensors can be fabricated using a variety of sensing materials, including semiconducting metal oxides, transition metal dichalcogenides (TMDCs), carbon nanomaterials (e.g., nanotubes and graphene-based materials), and others. The choice of sensing material influences the sensitivity and selectivity of the sensor towards specific gases. Resistive gas sensors are known for their simplicity of fabrication. They are cost-effective, making them suitable for various applications where inexpensive and easily producible sensors are required. Researchers have explored surface topography and chemical modification of sensing materials to enhance sensitivity to certain gases [4]. These modifications can improve the selectivity and response of the sensor. To generate sufficient working current and minimize output fluctuations, resistive gas sensors may need to be larger compared to other semiconductor-based sensors. The larger sensing area contributes to improved sensitivity but may require a larger heater to boost the operating temperature. Due to the need for a larger heater with a considerable sensing area, resistive gas sensors may consume more power to achieve and maintain the required operating temperature.

Optical gas sensors typically consist of three main components: a gas chamber, a light source, and a light detector. At a given light source wavelength, each gas has unique absorption characteristics. Hence, the specific wavelength of light emitted by the light source is selectively absorbed by the target gas molecules, allowing for detection and measurement using the light detector [5]. These sensors provide excellent stability owing to their minimal output drift and extended lifespan, as their working principle is solely based on the physical characteristic of the gas being sensed and does not include any chemical interaction between the optical sensor and the target gas molecules [6].

Additionally, they possess a high degree of selectivity and have rapid response times. Nevertheless, they include drawbacks in terms of miniaturization, high cost, and limited portability, hence restricting their industrialization and necessitating future enhancements. Additionally, ambient light interference affects them.

Electrochemical gas sensors comprise an electrolyte solution, a counter electrode, and a working electrode. These sensors detect target gases by detecting the potential difference or current between the two electrodes, which is produced by an oxidation or reduction process on the working electrode [7]. These sensors have high sensitivity to the gases being sensed even at low concentrations and may be operated using minimal power [8]. In addition, they are inexpensive and resistant to changes in surrounding humidity. However, electrochemical sensors are limited in their operational temperature range due to the possibility of the electrolyte solution drying up in high temperatures or low humidity conditions. These components have a limited lifespan and require regular calibration and maintenance of the electrolyte solution.

Surface Acoustic Wave (SAW) Sensors: When the gas molecules are adsorbed on the surface of the substrate, the changes in mass, viscoelastic properties, or frequency of the surface acoustic wave are measured [9][10]. They have disadvantages in terms of miniaturization, low portability, complex circuitry, and high cost.

Calorimetric Gas Sensors: These sensors utilize catalytic reactions to measure the concentration of gases. They are commonly used for combustible gas detection and operate by detecting changes in the rate of catalytic reactions (heat evolved) on a heated surface [11][12].

FET-type gas sensors employ a sensing material as the channel, which undergoes a threshold voltage shift or a change in drain current when exposed to the target gas [13]–[16]. These types of gas sensors cater to different applications and industries, ranging from industrial safety and environmental monitoring to healthcare and consumer electronics.

The choice of a gas sensor depends on factors such as the target gas, sensitivity requirements, and the operating environment. Advances in sensor technologies continue to drive innovation, enabling more accurate and reliable gas detection across various domains. The fabrication process begins with the careful selection of sensing materials, which can be organic or inorganic in nature, depending on the intended application [17]. The chosen materials are then processed and integrated into a sensor platform using various techniques such as thin-film deposition, printing technologies, or nanomaterial synthesis. The design and structure of the sensor are crucial to its sensitivity, selectivity, and overall performance [18]. In recent years, advancements in nanotechnology and material science have significantly contributed to the improvement of gas sensor fabrication [19]. Nanomaterials, such as graphene, metal oxides, 2-D materials, and carbon nanotubes, exhibit unique properties that enhance sensor performance, including high surface area, excellent conductivity, and sensitivity to specific gas species [20]. Gas sensors are fabricated through a combination of advanced materials, cutting-edge technologies, and intricate design processes. The fabrication of gas sensors involves the integration of sensitive materials capable of selectively interacting with specific gas molecules. This selectivity is vital for accurately identifying and quantifying the concentration of target gases in a given environment [21]. Additionally, the miniaturization of gas sensors has been a key focus in fabrication processes. Micro- and nano-scale sensors not only require smaller quantities of sensing materials but also enable the development of portable and wearable devices for personal gas monitoring. This trend has expanded the reach of gas sensor technology beyond traditional industrial applications, finding relevance in healthcare, agriculture, and even consumer electronics. As environmental concerns grow and the need for real-time monitoring increases, ongoing research in gas sensor fabrication continues to explore novel materials, fabrication techniques, and sensor designs. The ultimate goal is to develop highly sensitive, selective, and cost-effective sensors that can contribute to a safer and healthier living environment. This introduction sets the stage for delving deeper into the various aspects of gas sensor fabrication, exploring the latest innovations and their impact on diverse fields.

1.3 Hydrogen Sulfide: Characteristics and Dangers

Hydrogen sulfide (H_2S) is a colorless, highly toxic gas with a distinct, foul odor reminiscent of rotten eggs. Despite its offensive smell, its potency in terms of toxicity can be dangerously deceptive [22]. This section delves into the properties of hydrogen sulfide, its sources in different industries and natural processes, the associated health hazards, and the regulatory standards and guidelines governing permissible H_2S levels.

Properties of Hydrogen Sulfide: Hydrogen sulfide is a diatomic molecule composed of two hydrogen atoms and one sulfur atom (H_2S). It is a gas at room temperature and standard pressure, and its physical and chemical properties make it a unique and potentially hazardous substance [23].

Physical Properties:

- H_2S is slightly soluble in water, which means it can dissolve to some extent, leading to the formation of hydro sulfuric acid.
- It is denser than air, allowing it to accumulate in low-lying and confined spaces.

Chemical Properties:

- Hydrogen sulfide is a reducing agent and can react with metals to form metal sulfides.
- It can undergo combustion to produce sulfur dioxide and water.

Sources of Hydrogen Sulfide: Hydrogen sulfide is generated through both natural and anthropogenic processes, contributing to its presence in various environments [22].

Natural Sources:

- Volcanic Activity: H_2S is released during volcanic eruptions.
- Biological Processes: Anaerobic bacteria in natural environments produce hydrogen sulfide during the decay of organic matter.

Anthropogenic Sources:

- Industrial Processes: Oil and gas refining, petrochemical manufacturing, and pulp and paper production release H_2S.
- Waste Treatment: Sewage treatment plants produce hydrogen sulfide as a byproduct.
- Mining Activities: Extraction processes, particularly in the mining of sulfide ores, release hydrogen sulfide.

Health Hazards Associated with Exposure to Hydrogen Sulfide:

Exposure to hydrogen sulfide poses severe health risks due to its toxic effects on the respiratory and nervous systems [23]–[25].

Acute Health Effects:

- Respiratory Irritation: Even low concentrations can cause irritation of the eyes, nose, and throat.
- Nausea and Headaches: Higher concentrations lead to nausea, headaches, dizziness, and vomiting.
- Neurological Effects: At elevated levels, H_2S can affect the central nervous system, causing confusion and loss of consciousness.

Chronic Health Effects:

- Reproductive Effects: Long-term exposure may lead to reproductive toxicity.

- Neurological Disorders: Prolonged exposure may contribute to chronic neurological disorders.

Regulatory Standards and Guidelines for Permissible H_2S Levels: Recognizing the potential dangers of hydrogen sulfide exposure, regulatory bodies have established standards and guidelines to protect workers and the public.

Occupational Exposure Limits (OELs):

- Various organizations, including the Occupational Safety and Health Administration (OSHA) in the United States and the Health and Safety Executive (HSE) in the United Kingdom, have set permissible exposure limits for H_2S in workplace environments.

Environmental Standards:

- Regulatory agencies, such as the Environmental Protection Agency (EPA), set emission standards for industries to limit the release of hydrogen sulfide into the atmosphere.

Emergency Response Guidelines:

- Emergency response agencies provide guidelines for dealing with accidental releases of hydrogen sulfide, emphasizing prompt evacuation and proper protective measures.

1.4 Introduction to Organic Semiconductors

Organic polymer semiconducting (SC) materials have several benefits over standard inorganic SC materials, including the ability to be produced at ambient temperature and being lightweight and inexpensive [1]. They are also soluble in various organic solvents and can be easily deposited onto the substrates, demonstrating excellent solution-processibility [26]. In some respects, this makes them competitive with gallium arsenide and silicon. Organic semiconductors have various benefits because they are easy to process and compatible with a wide range of substrates, including flexible plastic substrates, and due to the tailorable structure of organic semiconductors. Solution-processed organic semiconductors have the advantage of being able to be processed at low temperatures. Moreover, organic semiconductor thin films provide excellent mechanical robustness as well as flexibility. This allows them to be used with plastic substrates, which cannot handle the high-temperature processing needed for traditional thin film inorganic semiconductors. Furthermore, the ability to fabricate organic devices using low-temperature solution processing opens up multiple avenues for low-cost and high-volume production. The ability to tune semiconductor characteristics through modification of their molecular structure also permits potentially tailor-made molecules for specific device applications. In several electronic devices, including organic field effect transistors (OFET), solar cells, photodetectors, and organic light-emitting diodes (OLED), organic materials have been extensively employed. One of the most appealing domains for scientific investigation is OFETs [2][27].

The history of organic semiconductors is a fascinating journey marked by significant milestones and breakthroughs in material science and electronics. This narrative unfolds over the course of several decades, tracing the evolution of organic semiconductors from their discovery to their diverse applications in modern technology. Here is a chronological overview of the key milestones in the history of organic semiconductors:

1. Early Discoveries (Late 19th to Early 20th Century): The exploration of organic semiconductors began with the discovery of organic compounds exhibiting semiconducting properties. Early researchers observed that certain organic materials, such as dyes and pigments, could conduct electricity to some extent.

2. Rise of Conducting Polymers (1970s): The field gained momentum in the 1970s with the discovery of conducting polymers. Researchers, including Alan J. Heeger, Alan G.

MacDiarmid, and Hideki Shirakawa, demonstrated that certain polymers, such as polyacetylene, could exhibit metallic conductivity upon doping. This discovery earned them the Nobel Prize in Chemistry in 2000.

3. Organic Light-Emitting Diodes (OLEDs) (1987): The development of organic semiconductors took a leap forward with the invention of organic light-emitting diodes (OLEDs). Ching W. Tang and Steven Van Slyke demonstrated efficient electroluminescence in organic thin films, paving the way for the commercialization of OLED displays and lighting.

4. Organic Thin Film Transistors (OTFTs) (1990s): The 1990s witnessed the emergence of organic thin film transistors (OTFTs). Researchers explored the use of organic semiconductors in transistors, enabling the fabrication of flexible and lightweight electronic devices.

5. Organic Photovoltaics (Early 2000s): The early 2000s saw a surge of interest in organic photovoltaics (OPVs). Researchers aimed to harness the unique properties of organic semiconductors for solar cell applications. Efforts were made to improve the efficiency and stability of organic solar cells.

6. Progress in Organic Electronics (2000s-2010s): Organic electronics gained traction with advancements in materials and fabrication techniques. Organic semiconductors have found applications in various devices, including sensors, memory devices, and wearable electronics. The field expanded beyond traditional silicon-based electronics.

7. Flexible and Printed Electronics (2010s-Present): The 2010s marked a significant era for organic semiconductors in the realm of flexible and printed electronics. These materials allowed the development of bendable and stretchable electronic devices, enabling innovative applications in healthcare, wearables, and IoT devices.

8. Continued Exploration and Future Prospects: Research and development in the field of organic semiconductors continue to explore new materials and applications. On-going efforts focus on improving the performance, stability, and scalability of organic electronic devices. Challenges like stability, reproducibility, and achieving high carrier mobility in organic semiconductors continue to be areas of active research. The future holds promise for sustainable and low-cost electronics, advanced organic materials, new fabrication techniques, and expanded applications in emerging technologies.

In conclusion, the history of organic semiconductors is characterized by a series of pivotal discoveries and advancements that have transformed the landscape of electronics. From the early exploration of conducting polymers to the widespread adoption of OLEDs, OTFTs, and the development of flexible electronics, organic semiconductors have played a crucial role in shaping the future of electronic technologies. The journey is ongoing, with researchers pushing the boundaries of material science and engineering to unlock new possibilities in the world of organic electronics.

1.4.1. Bonding in Organic Semiconductors

The bonding properties of organic semiconductors differ particularly from those of their inorganic counterparts. The first polymer with conducting capabilities to be described was polyacetylene. In terms of their electrical characteristics and molecular structure, organic semiconductors are unique. Organic polymers containing alternating single and double bonds along the polymer chain are known as conjugated polymers [28]. The typical representation of this alternate arrangement is shown in **Figure 1.1.** This double bond conjugation facilitates electron delocalization, forming a system of π-electron clouds parallel to the polymer backbone. These conjugated double bonds provide the polymer with unique electronic characteristics and electrical conductivity [29]. However, doping is frequently necessary to improve and regulate this conductivity. Doping is the process of introducing certain chemicals into a polymer in order to change its electrical structure. p-type doping and n-type doping are the two primary forms of doping. An oxidizing substance is employed in p-type doping to extract electrons from the conjugated polymer, resulting in "holes" in the electron structure [30]. The material's electrical conductivity is enhanced by these holes, which serve as positive charge carriers. A reduction agent is added to the conjugated polymer to increase its electron count in n-type doping. The material's electrical conductivity is enhanced by the extra electrons, which also raise the electron density [31]. The electrical characteristics of the conjugated polymer may be precisely tuned for a variety of uses, including organic electronics, solar systems, and sensors, by carefully managing the doping process. In the realm of organic electronics, conjugated polymers are useful materials because of their doping-based capacity to modify conductivity.

Figure 1.1 The Molecular structure of the polyacetylene.

Now, let's discuss the bonding characteristics in the alternating single and double bonds of conjugated polymers. A sigma bond (σ) is formed when two s-orbitals overlap end-to-end, allowing the sharing of electrons. It is the strongest type of covalent bond and is characterized by the direct head-on overlap of atomic orbitals. In the context of the alternating single and double bonds in conjugated polymers, the single bonds are sigma bonds. A π- bond is formed when two p-orbitals overlap side by side, creating a region of electron density above and below the plane of the atoms. In the case of double bonds in conjugated polymers, the π bond is formed alongside the sigma bond. The π bond arises from the overlap of p-orbitals that are perpendicular to the plane of the sigma bond. The formation of π bonds involves the excitation of electrons. In the case of carbon atoms undergoing sp^2 hybridization (see **Figure 1.3**), one electron from the 2s orbital is excited to the p_z orbital, resulting in three sp^2 hybrid orbitals. The sp^2 hybridization allows for the formation of sigma bonds with other atoms and the creation of the π bond in the conjugated system.

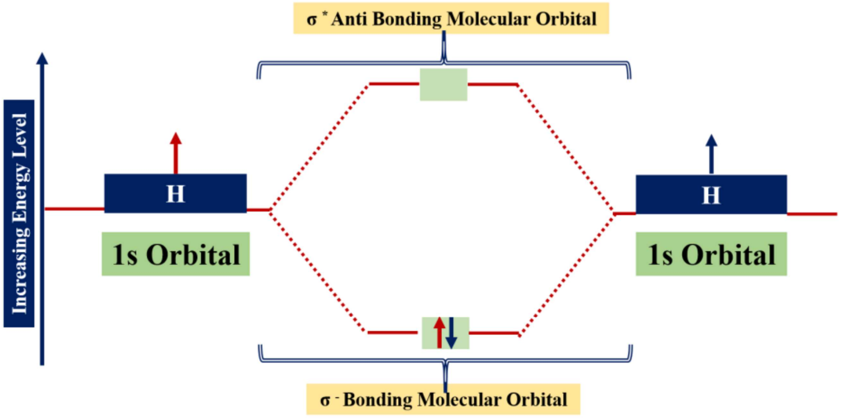

Figure 1.2 σ-bonding and $\sigma*$-antibonding formation.

Let's summarize and elaborate on the key points:

π-Bonds and Electron Sharing: π-bonds result from the direct sharing of a pair of electrons between the p_z-orbitals of adjacent carbon atoms in a conjugated system. Unlike σ-bonds, which are formed by head-on overlap of orbitals, π-bonds involve side-by-side overlap of p_z -orbitals.

Strength of π-Bonds: π-bonds exhibit less strength compared to σ-bonds. This is attributed to the greater spatial separation of the p_z -orbitals from the positively charged nucleus. The weaker nature of π-bonds allows for easier disruption, contributing to the dynamic and responsive nature of conjugated polymers.

Electron Localization in π-Bonds: During the formation of π-bonds, electron localization occurs. This means that the electrons are concentrated in the region between the carbon atoms participating in the π-bond. This localization is a consequence of the spatial distribution of the p_z -orbitals involved in π-bonding.

Conjugation and Electron Delocalization: Conjugated systems in polymers and oligomers involve the presence of alternating single and double bonds, creating a chain of conjugated π-electron systems. The π-orbitals have the ability to overlap not only within a molecule but also with adjacent molecules, promoting electron delocalization. Electron delocalization allows charge carriers (electrons or holes) to move freely along the polymer chain or between adjacent molecules.

Conduction in Polymers: The phenomenon of charge carriers being delocalized along the chain of the polymer is crucial for the electrical conductivity of conjugated polymers and oligomers. This delocalization of charge carriers enables the efficient transport of electrical charge, making these materials conductive. Understanding the interplay between σ-bonds and π-bonds, as well as the concept of electron delocalization, provides insight into the unique electronic and conductive properties of conjugated polymers [32].

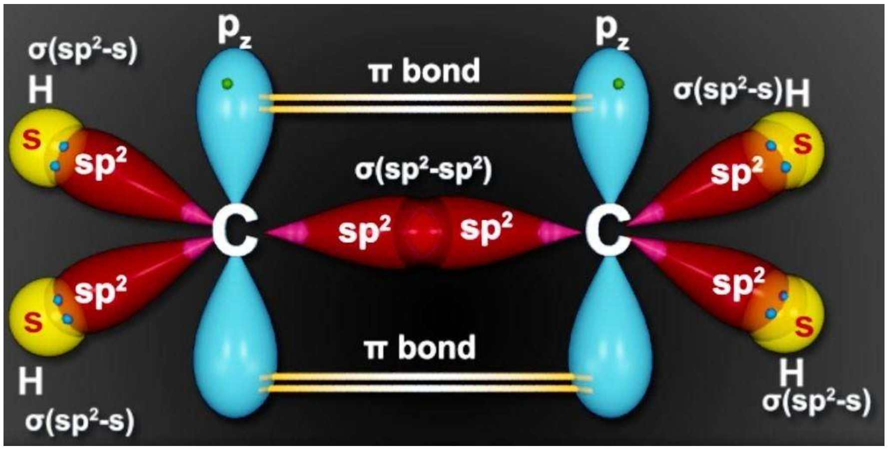

Figure 1.3 sp^2 *hybridization.*

Consequently, the presence of a repetitive arrangement of alternating single and double bonds inside a conjugated molecular framework gives rise to bonding and anti-bonding electronic states. Using H_2 as a case study, σ-bonding and σ* antibonding have been depicted in **Figure 1.2** above. This arrangement also leads to the formation of a forbidden energy gap between spatially delocalized electronic band structures. Please refer to **Figure 1.4** shown below-

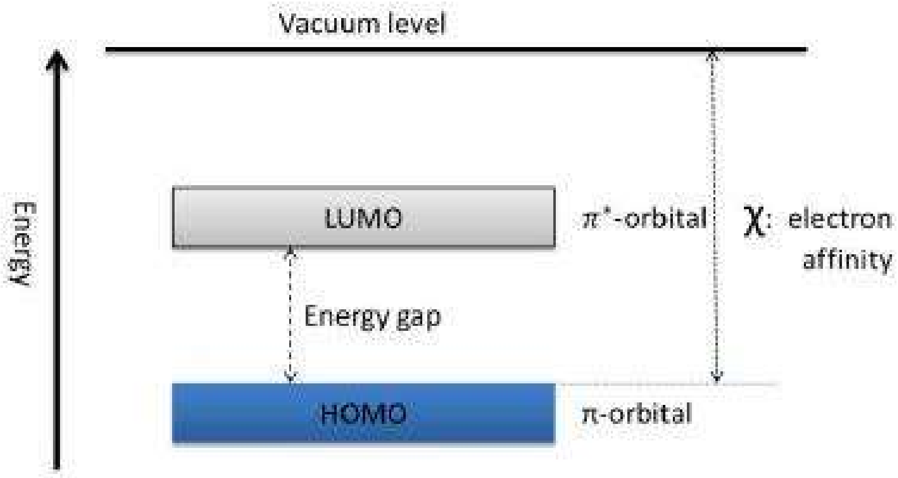

Figure 1.4 HOMO, LUMO, and Energy bandgap of organic polymer.

1.4.2. Energy Level in Organic Semiconductors

Optimizing the energy levels of molecular orbitals in a polymer is crucial for achieving effective alignment with the work function of metal electrodes. Proper alignment enhances the efficiency of charge carrier injection and transport at the polymer-metal interface.

HOMO (Highest Occupied Molecular Orbital): This orbital consists of π-orbitals with electrons in a bonding state. It is analogous to the valence band in inorganic semiconductors.

LUMO (Lowest Unoccupied Molecular Orbital): This orbital consists of π*-orbitals with unpaired electrons in an anti-bonding state. It is analogous to the conduction band in inorganic semiconductors.

In the context of p-type and n-type semiconductors, the HOMO level is often observed to be around 5 electron volts (eV). The LUMO level typically falls within the range of 3 eV to 4 eV for these materials.

Band Gap (Eg): The energy difference between the HOMO and LUMO is defined as the band gap (Eg). It represents the energy required to move an electron from the highest occupied state to the lowest unoccupied state. The band gap is a critical parameter that influences the optical and electronic properties of the material. Optimizing the energy levels of molecular orbitals, understanding the HOMO and LUMO states, and controlling the band gap is essential for tailoring the electronic properties of conjugated polymers. This fine-tuning enables the design of polymer materials with specific functionalities, making them suitable for various applications in organic electronics and optoelectronics. As previously stated, the process of doping plays a crucial role in augmenting the conductivity of materials. This fundamental approach is used to ascertain the semiconductor characteristics, specifically if they are of the p-type or n-type. Electron affinity, also known as ionization potential, is a significant characteristic that determines the stability of materials under ambient conditions.

1.4.3. Advantages of Organic Semiconductors

A qualitative study was performed in this section in order to examine the merits and demerits of organic semiconductors in comparison to inorganic semiconductors. **Table 1.1** presents a comprehensive overview of the key factors that are crucial for evaluating the quality of organic semiconductors. Organic semiconductors have several benefits, including low-temperature fabrication, cost-effectiveness, and the ability to form flexible films [33]. However, they exhibit lower mobility and inferior stability when compared to their inorganic semiconductor counterparts. **Table 1.1** presents an in-depth comparison of organic semiconductors and inorganic semiconductors across several characteristics [33][29].

Table 1.1 Comparison between Organic and Inorganic semiconductors

Comparison table of Organic/Inorganic semiconductors		
Parameters	**Organic semiconductors**	**Inorganic semiconductors**
Processing Temp.	Low Temperature	Mostly High Temperature
Flexibility	Flexible	Inflexible
Stability	Less Stable	Highly Stable
Mobility	Low Mobility	High Mobility
Transparency	Less Transparent	Highly Transparent
Differences in terms of various Electrical parameters		
Charge Transport	Hoping	Band to Band
Carrier Mobility	~1 $cm^2/V.$ sec.	~1000 $cm^2/V.$ sec.

1.4.4. Organic Thin Film Deposition Methods

Organic semiconducting polymers are commonly used in the fabrication of thin films for various electronic devices, such as organic solar cells, organic light-emitting diodes (OLEDs), and organic field-effect transistors (OFETs). The choice of the fabrication method depends on factors such as the desired film properties, the specific application, and the scalability of the process. Researchers and engineers often optimize the deposition method based on the requirements of the organic electronic device they are fabricating. This section will cover the different techniques for the growth of the thin film over the various substrates. Here are some common solution-processed methods for fabricating thin films of organic semiconducting polymers-

Spin Coating: Spin coating is a widely used technique for depositing uniform thin films of organic semiconducting polymers. In this method, a solution of the polymer is applied to a substrate, which is then spun at high speeds to spread the solution evenly. The excess solution is then spun off, leaving behind a thin, uniform film [34][35].

Drop Casting: In drop casting, a solution of the organic semiconductor is simply dropped or dispensed onto a substrate. The solution is allowed to spread and dry, forming a thin film. This method is relatively simple but may not provide the same level of control over film thickness and uniformity as spin coating [36].

Doctor Blade Coating: Doctor blade coating, also known as blade coating or knife coating, involves spreading a solution of the organic semiconductor onto a substrate using a blade. The blade controls the thickness of the resulting film, and excess solution is scraped away. This method is suitable for large-area film deposition [37].

Inkjet Printing: Inkjet printing allows for the precise deposition of small droplets of a solution containing the organic semiconductor onto a substrate. This method is advantageous for its ability to pattern materials with high spatial resolution, making it useful for the fabrication of organic electronic devices [38].

Slot-Die Coating: Slot-die coating is a continuous and scalable method for depositing thin films. In this technique, a solution is pumped through a narrow slot and deposited onto a moving substrate. The film thickness is controlled by adjusting the gap between the slot die and the substrate [39].

Spray Coating: Spray coating involves spraying a solution of the organic semiconductor onto a substrate. This method is suitable for large-area deposition and can be used to achieve relatively uniform films [40].

Langmuir-Blodgett Technique: The Langmuir-Blodgett technique involves the deposition of a monolayer of organic molecules or polymers from the air-water interface onto a solid substrate. This method is particularly useful for achieving highly ordered and oriented thin films [41].

Dip Coating: Dip coating involves immersing a substrate into a solution of the organic semiconductor and then withdrawing it at a controlled rate. The withdrawal speed and solution properties influence the film thickness [42].

Floating Film Transfer (FTM) Method: The FTM (Floating Film Transfer Method) is a growth technique that involves the self-assembly of polymer films at the interface between polymer solution and liquid substrate. This technology has demonstrated several advantages, including its simple fabrication procedure, low material wastage, and suitability for large-scale production on various substrates [43]. The FTM approaches provide precise control over the ordering of polymer chains, the crystalline behavior, and the thickness of the self-oriented layer on the substrate. This approach has mostly been optimized for polymers belonging to the thiophene family, such as P3HT, PBTTT, PCPDTBT, and PQT-12 [44].

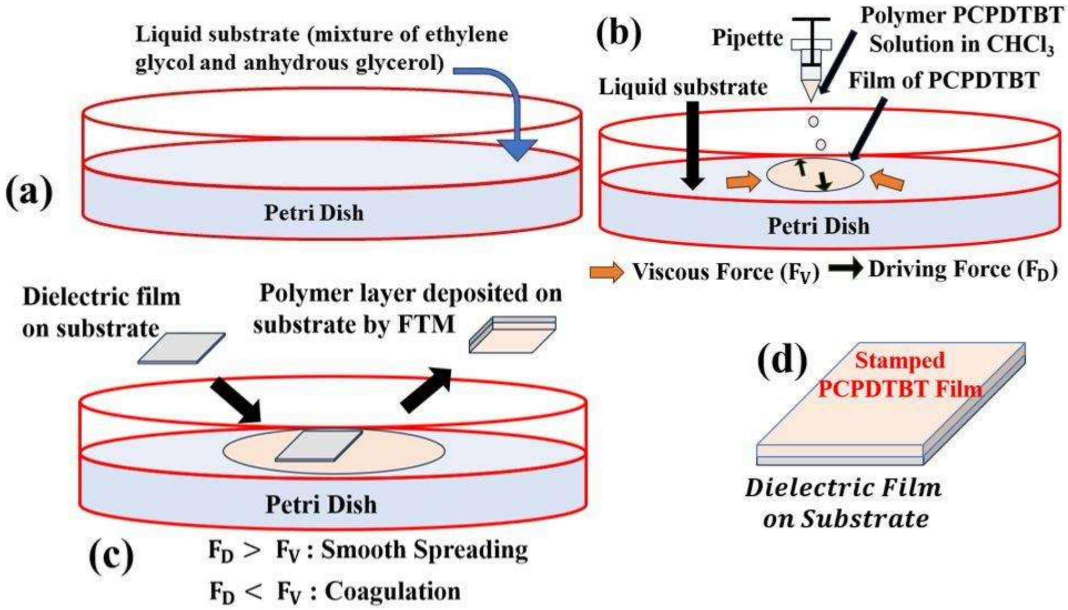

Figure 1.5 Floating film transfer methods, (a) Nucleation growth of the polymer thin film (suitable for film deposition), (b) Coagulated thin film (not suitable for film deposition), (c) Thin film transfer over the hydrophobic substrate.

The self-assembly of these thiophene derivatives is facilitated by the regio-regular grafting of an alkyl side chain, which minimizes steric hindrance during thin film production.

The growth of polymer crystals in a floating film on a liquid substrate is influenced by various factors, such as the solubility of polymers in nonpolar solvents, the surface free energy of the solvent, the density fluctuation, the relative viscosity, relative thermal conductivity, the evaporation flux, the temperature gradient, and the spreading coefficient [45]. Initially, concentrate on the surface energy required for the formation of pure polymer over a liquid substrate consisting of a 1:1 ratio of ethylene glycol to glycerol. **Figure 1.5** depicts an elementary schematic.

As per the principle of Marangoni flow, it is observed that a solvent with a lower surface energy would exhibit a natural tendency to disperse over a solvent having a higher surface energy [45]. The flow theory has been employed in this study to facilitate the self-assembly and oriented development of the PCPDTBT conductive polymer on a liquid substrate composed of a 1:1 ratio of Ethylene Glycol and Glycerol. At the interface between the adjacent materials, the surface pressure gradient arises due to the introduction of a low surface energy solvent (specifically, PCPDTBT in chloroform solution in our study) onto a high surface energy solvent. This surface pressure gradient induces the spontaneous spreading of the low surface energy solvent towards the highly stressed surface, as depicted in **Figure 1.5 (c).**

In the context of the spontaneous development of thin films, two forces are at play: the driving force and the viscous force. The nucleation development of the film over the liquid substrate, which has a high surface energy, is primarily driven by a driving force. On the other hand, the spontaneous spreading of the film is hindered by a counteracting force known as the viscous force. The effective spreading force (F_{ES}) in the context of the spreading equation is determined by the difference between the driving force (F_D) and the viscous force (F_V). This equation governs the nucleation development of the film. Additionally, the spreading coefficient for the thin film may be expressed as.

$$\gamma = \gamma_1 - \gamma_2 - \gamma_{12} \tag{1.1}$$

γ_1 – Surface tension of the liquid substrate effective towards the outside

γ_2 – Surface tension of the polymer solution in chloroform effective towards the inside

γ_{12} – Signifies the surface tension developed at the interface boundaries of the liquids

The production of an air-processable, self-assembled, large-area thin film over a liquid substrate is only achievable with the combination of rapid evaporation and simultaneous solidification of the polymeric solution. In order to achieve the spreading of the polymer solution across the liquid hydrophobic substrate, it is necessary for the driving force to exceed the viscous force [45]. Put simply, it is necessary for F_{ES} to have a value larger than zero, denoted as $F_{ES}>0$. In the event that the driving force is insufficient in comparison to the viscous force, the nucleation spreading of the polymer solution becomes unattainable. Alternatively, the spreading process results in the formation of a coagulated or drop structure, as seen in **Figure 1.5 (b).** The fabrication of a compact, high-quality, self-assembled polymer thin film may be achieved by optimizing the concentration of the polymeric solution and the concentration of the liquid subphase/substrate. This approach enables the production of a large area of thin film. The thin layer that covers the hydrophobic liquid subphase/substrate may be readily stamped onto any hydrophobic substrate, as seen in **Figure 1.5 (c). Figure 1.5** illustrates the comprehensive mechanisms involved in the film spreading and film lifting phenomena occurring on the hydrophobic substrate.

1.5 Gate Dielectrics in TFTs

Replacing silicon dioxide (SiO_2) with high-k dielectrics in semiconductor devices, such as metal-oxide-semiconductor field-effect transistors (MOSFETs), is driven by several key factors. While SiO_2 has been the traditional choice for gate dielectrics due to its excellent insulating properties, the need for alternative high-k dielectrics arises due to the following challenges:

Gate Leakage Currents: As the size of semiconductor devices shrinks, it becomes necessary to reduce the thickness of the SiO_2 gate dielectric layer in order to ensure sufficient control over the transistor. Nevertheless, thin SiO_2 layers have a susceptibility to elevated leakage currents, resulting in increased power consumption and decreased energy efficiency [46].

Quantum Tunnelling Effects: Quantum tunneling emerges as a significant concern within very thin SiO_2 layers. The phenomenon of electron tunneling through the thin SiO_2 barrier might result in unexpected behavior and compromise the stability of the transistor [47].

Threshold Voltage Variability: Thickness variation in SiO_2 layers, particularly at microscale dimensions, can lead to variations in threshold voltage among transistors. The presence of inconsistencies in device characteristics is considered unfavorable in the context of integrated circuits that strive for excellent reliability as well as performance.

Higher Capacitance Requirements: In order to retain gate capacitance while simultaneously decreasing the thickness of the dielectric, it becomes necessary to employ materials possessing higher dielectric constants, sometimes referred to as high-k materials. High-k dielectrics enable the utilization of thicker dielectric layers while maintaining capacitance, hence mitigating leakage currents and enhancing transistor performance [48].

Increased Heat Generation: Reduced thickness of SiO_2 layers is associated with enhanced electric field intensity, leading to elevated thermal energy within the transistor. The elevated temperature has the potential to adversely affect the stability of electronic devices and escalate the likelihood of thermal failure.

In summary, the need to replace silicon dioxide with high-k dielectrics arises from the limitations associated with scaling down SiO_2-based gate dielectrics. High-k materials offer a solution by providing improved insulating properties, reduced leakage currents, and enhanced compatibility with advanced semiconductor manufacturing processes. These advancements contribute to the ongoing progress in semiconductor technology and the development of more efficient and powerful electronic devices.

1.5.1. Classification of Gate Dielectrics

The categorization of gate oxide dielectrics is presented in **Figure 1.6**. Various dielectrics provide unique advantages and disadvantages. **Table 1.2** provides a comprehensive summary of the attributes shown by several classifications of dielectric materials. This thesis primarily focuses on the application of inorganic dielectrics with high-k values and wide-band gaps in the manufacturing process of organic thin-film transistors (TFTs).

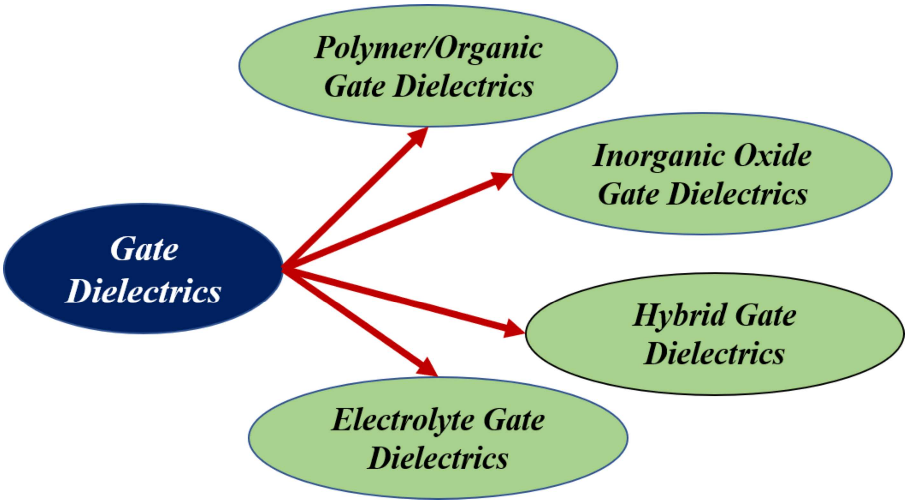

Figure 1.6 Classification of gate dielectric materials.

Table 1.2 Difference between various types of Dielectric Materials

Gate Dielectrics	Properties
Inorganic Oxide Gate Dielectrics	❖ Usually belong to the IIA, IIIA, IIIB, IVB, and VB group Metal Oxides. ❖ High dielectric constant. ❖ Generally, it requires a high temperature for synthesis. ❖ Inorganic Oxides are brittle in nature. ❖ High dielectric strength. ❖ Mechanical inflexibility/Brittle in nature.
Organic/Polymer Gate Dielectrics	❖ Low dielectric constant. ❖ Low-temperature solution processibility.

	❖ Mechanical flexibility. ❖ Smoother surface.
Hybrid Gate Dielectrics	❖ Usually consists of polymer/inorganic blend materials. ❖ High dielectric constant with mechanical flexibility. ❖ High surface smoothness.
Electrolyte Gate Dielectrics	❖ Consists of ion gels, ionic liquids, polyelectrolytes, and electrolytes.

1.5.2. Selection Criteria of the Gate Dielectrics

The selection of high-k dielectrics for thin-film transistors (TFTs) necessitates the careful evaluation of several criteria in order to get the most favorable performance of the transistors. Key selection parameters for high-k dielectrics in thin-film transistors are as follows:

Dielectric Constant (k): High-k (should be in the range of 10 - 30) materials are selected based on their higher dielectric constants. A higher dielectric constant enables the utilization of a thicker dielectric layer while maintaining capacitance, hence mitigating leakage currents and enhancing the overall performance of transistors [46].

Capacitance and Gate Oxide Thickness: The utilization of high-k dielectrics facilitates the production of thin gate dielectric layers while sustaining the necessary capacitance. The aforementioned factors are of utmost importance in attaining optimal transistor performance, mitigating leakage currents, and enhancing the transistor's on/off ratio.

Energy Band Gap and Band offset: The dielectric/oxide materials should possess excellent insulating properties, characterized by a band gap (Eg) of more than 5 eV. Additionally, it is necessary to have a significant band offset (E_{offset}) between the interface of silicon (Si) and the dielectric material, with a value above 1 eV. This requirement is particularly important when depositing the dielectric material onto a silicon substrate [46].

Thermal Stability: The selected high-k dielectric material should demonstrate favorable thermal stability during the fabrication process and subsequent operation of the device. This indicates that the dielectric characteristics remain constant throughout the operational lifespan of the device.

Chemical Compatibility: The compatibility of high-k dielectrics with the fabrication processes employed in thin-film transistor fabrication is of utmost importance. Ensuring chemical compatibility is crucial in order to prevent unfavorable reactions with other substances within the transistor stack.

Carrier Mobility and Charge Trapping: The influence of the dielectric material on the carrier mobility of the semiconductor layer should be minimal. Furthermore, it is imperative for the dielectric to reduce the occurrence of charge-trapping effects in order to uphold the consistency of transistor performance [48].

Breakdown Voltage: In order to resist the electric field stress that occurs during transistor operation, it is vital for high-k dielectrics to possess a breakdown voltage of significant magnitude.

Process Compatibility: It is imperative that the high-k dielectric material exhibits compatibility with the deposition procedures and processing conditions employed in the fabrication of thin-film transistors.

Cost and Scalability: The cost and scalability of high-k dielectric material for large-scale manufacturing are crucial. Cost-effective and scalable materials are essential for thin-film transistor commercialization.

Surface Passivation: High-k dielectrics have the capability to function as efficient surface passivation layers, therefore safeguarding the underlying semiconductor material against various environmental influences. Additionally, they play a crucial role in avoiding the entrapment of charge carriers at the interface between the semiconductor and dielectric.

Frequency Response: The dielectric characteristics should be able to support efficient charge transfer and limit parasitic capacitance in order to enable faster switching rates for applications that need a high-frequency operation.

Selecting the right high-k dielectric for thin-film transistors involves a careful balance of these criteria to optimize device performance, reliability, and manufacturability. The specific requirements may vary depending on the application and performance goals of the thin-film transistor. The relation between the inorganic dielectric constant (k) and the band gap is plotted in **Figure 1.7**. It clearly illustrates that there is an inverse relationship between the band gap and dielectric constant in the inorganic dielectric materials.

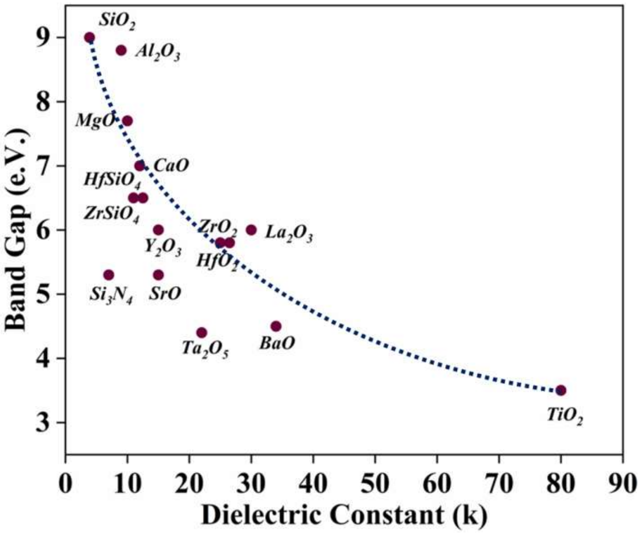

Figure 1.7 Bandgap vs. dielectric constant of standard gate dielectric materials.

According to **Figure 1.7,** it can be observed that the dielectric materials ZrO_2, HfO_2, and La_2O_3 exhibit superior characteristics and are hence considered the optimal options for gate dielectric materials. However, a notable drawback of La_2O_3 is its susceptibility to a pronounced reaction with water vapor or moisture. This reaction adversely affects the overall performance of the device, particularly in terms of relative stability, due to its sensitivity to humid conditions. Therefore, it can be concluded that ZrO_2 and HfO_2 exhibit superior characteristics as gate dielectric materials, possessing a high-k value of around 25 in their original state (refer to **Figure 1.8**).

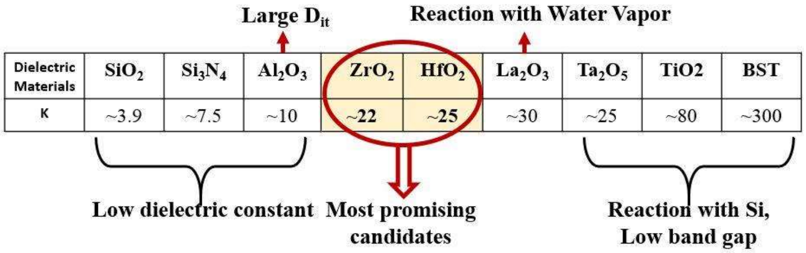

Dielectric Materials	SiO_2	Si_3N_4	Al_2O_3	ZrO_2	HfO_2	La_2O_3	Ta_2O_5	TiO2	BST
K	~3.9	~7.5	~10	~22	~25	~30	~25	~80	~300

Figure 1.8 Selection of promising candidates for the gate oxide/dielectric film in TFTs.

1.5.3. Deposition Methods of Inorganic Oxide Dielectrics in TFT Fabrication

Presently, the deposition of inorganic dielectric films is commonly achieved by the utilization of gas phase and processible solution technologies. Gas phase deposition technologies, such as atomic layer deposition (ALD), pulsed laser deposition (PLD), and chemical vapor deposition (CVD), are characterized by their lengthy processing times and high costs. However, these processes provide distinct advantages in terms of the quality of dielectric films produced, surpassing those achieved using solution-based deposition techniques such as spray coating, dip coating, and spin coating. In our study, thermal oxidation and low-cost spin coating techniques were employed to fabricate the gate oxide layer. The optimization of gate dielectric layer thickness in the solution-processed approach involves manipulating parameters such as rotation speed, spin time, and concentration of the dielectric solution throughout the manufacturing process.

1.6 Structures and Charge Transport Mechanism in OFETs

1.6.1. Architecture of OFETs

Transistor architectures may be categorized into two categories, namely top-gate and bottom-gate, depending on the gate deposition location. Each transistor has two kinds of electrodes, namely the source and drain electrodes, which are composed of distinct combinations of semiconductor layers. Hence, the overall count of structures amounts to four, each of which is visually shown in **Figure. 1.9** presented subsequently [49].

The aforementioned device architectures illustrate that a thin film transistor is controlled by three electrodes: the gate, drain, and source. In this context, it is imperative that the semiconductor layer maintains continuous contact with both the drain and source regions while being physically isolated from the gate region utilizing a layer of the dielectric. Structures (a) and (b) are the most widely favoured. In both instances, the organic semiconductor has the potential to be applied over the dielectric layer before the metallic electrode's deposition. This approach has demonstrated efficacy in enhancing the interface quality between the dielectric and semiconductor layers. The quality of the interface is a crucial aspect of the device fabrication process. The variation in characteristics observed in organic semiconductors developed on various kinds of substrates can significantly impact the performance of devices. The interface between these two layers exhibits a high degree of uniformity, hence minimizing the possibility of charge carrier trapping. In contrast, it is anticipated that the development of molecular crystals on two different materials, metal and dielectric material, will produce different structures and characteristics on these surfaces in the case of the other two structures. Consequently, this discrepancy is likely to obstruct the injection of charge carriers. The probable consequence of this action is a decline in the device's performance.

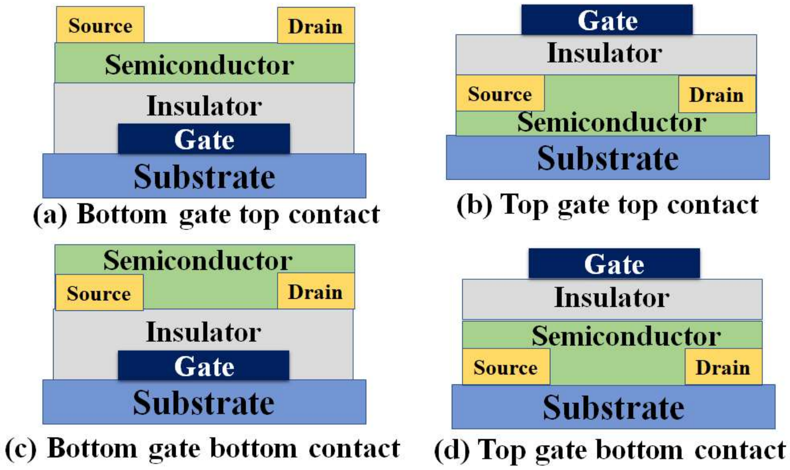

(a) Bottom gate top contact
(b) Top gate top contact
(c) Bottom gate bottom contact
(d) Top gate bottom contact

Figure. 1.9 Different architectures of organic thin film transistors.

The significance of the architecture of thin-film transistors (TFTs) in relation to their performance has been properly highlighted. **Table 1.3** provides a detailed overview of the features associated with various architectural designs [50][49].

Table 1.3 Advantages and Disadvantages of Different TFT Architectures

Device Architecture	Advantages	Disadvantages
Top Gate	❖ The gate and source/drain electrodes can be deposited on top of the device by printing processes or any other deposition techniques with high printing resolution. ❖ A gate insulator and a gate electrode on top of the active layer can provide an encapsulation effect against any environmental impact, increasing the device's stability. ❖ In top-gate TFTs, high-quality active layer films can be deposited on top of flat substrates, so the morphology of the active layer film is independent of the surface of the dielectric material.	❖ The top gate structure is challenging to fabricate. ❖ The surfaces of source/drain electrodes in a top gate bottom contact device may influence the film morphology. ❖ A compatible mask for the organic semiconductor layer is required.
Bottom Gate	❖ The bottom gate structure is straightforward in fabrication. ❖ Thermal annealing of the dielectric layer over the gate does not damage the Organic Semiconductor layer.	❖ Requires a proper passivation layer for the Organic semiconductor channel to enhance the stability and lifetime of the OTFT.
Top Contact	❖ The top contact structure offers lower contact resistance due to the channel's large injection area for charge carriers.	❖ Complex fabrication process and a chance of contact penetration in the deposited film.
Bottom Contact	❖ Suitable for low-cost, flexible electronic applications.	❖ High metal contact resistance. ❖ The presence of a barrier increases the subthreshold swing and lowers the field effect mobility.

1.6.2. Charge carrier Transport Mechanism.

A Thin-Film Transistor (TFT) has four essential components: a drain, gate, source, and active (channel) layer. The present dissertation incorporates an active layer, including a gas-sensitive material, which is utilized for the purpose of sensing applications. The charge carrier injection in thin-film transistors (TFTs) occurs through the source and drain terminals. These charge carriers then traverse the channel in a parallel manner to the gate insulator layer. The charge injection process may be elucidated by the alignment of the work function of the metal contact and the energy levels of the highest occupied molecular orbital (HOMO) and lowest unoccupied molecular orbital (LUMO), as seen in **Figure 1.10** [50]**.** The HOMO and LUMO bands of the conjugated polymer are associated with two electrodes positioned at the Fermi level. Taking the n-type as an illustrative instance, when the bias at the gate is set to zero, and even when a voltage is applied between the drain and source electrodes, no current is observed due to the absence of mobile charge carriers within the active sensing layer. As the bias at the gate is elevated, a significant electric field is generated at the interface between the organic polymer and insulating layers. The phenomenon under consideration induces a bending of the LUMO energy level band, resulting in its alignment relative to the Fermi level of the metal contact. This alignment occurs when the gate voltage exceeds a certain threshold, leading to a resonation between the LUMO energy and Fermi levels (known as the flat band condition) [50]. Furthermore, it should be noted that an accumulation of negative charges occurs inside the lowest unoccupied molecular orbital (LUMO) band before the application of a slight positive voltage. This phenomenon facilitates the flow of electric current from the source to the drain contacts.

In the case of p-type semiconductors, when a negative bias is applied to the gate, the highest occupied molecular orbital (HOMO) band will align and resonate with the electrodes at the Fermi level, provided that the negative gate voltage is of sufficient magnitude. Consequently, there will be a gradual accumulation of holes inside the HOMO band. The application of a relatively low voltage potential across the source and drain terminals generates an electric current within the semiconductor layer [50].

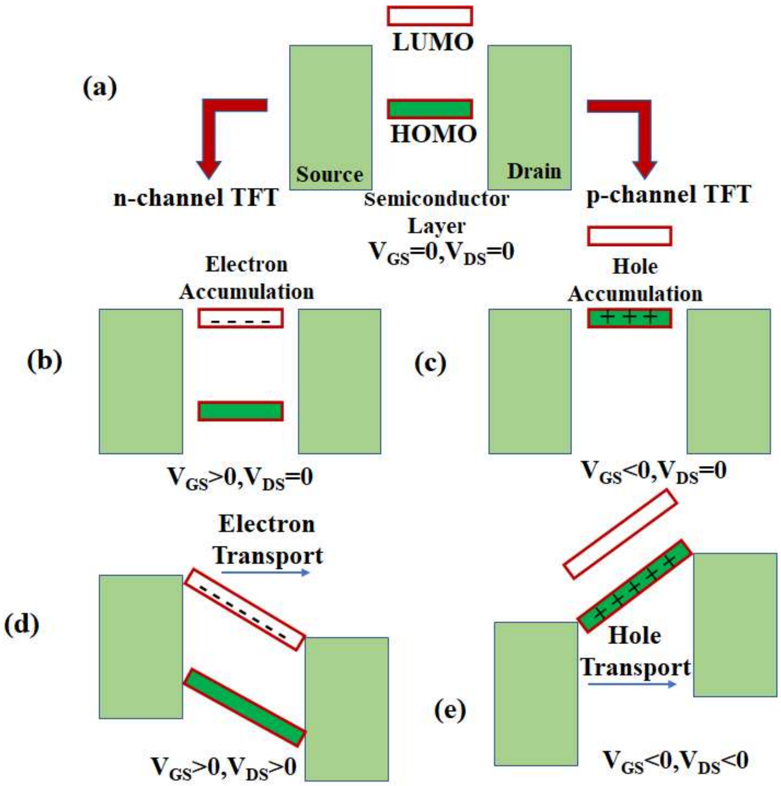

Figure 1.10 Thin film transistor operation on the application of electric field, (a) Ideal energy level diagram of TFT at V_{GS}=0, V_{DS}=0 (b) Electron accumulation at V_{GS}>0, V_{DS} =0, (c) Hole accumulation at V_{GS} <0, V_{DS} =0 (d) Electron transport at V_{GS}>0, V_{DS} >0, (e) Hole transport at V_{GS}<0, V_{DS}<0.

1.6.3. Current flow in an OFET

The magnitude of the source-drain current in an organic field-effect transistor (OFET) is directly influenced by the relative values of the gate voltage (V_{GS}) and the drain voltage (V_{DS}). Initially, it is necessary for the gate voltage to surpass a specific threshold voltage, denoted as Vth, in order to establish a charge carrier channel at the interface of the insulator. Organic Field-Effect Transistors (OFETs) have the capability to function within three distinct current regimes, including the linear regime, the pinch-off point, and the saturation regime [50]. **Figure 1.11(a)** illustrates the linear operation regime. In the scenario where the source is grounded, if the voltage difference between V_{GS} and V_{th} is significantly more than V_{DS}, it can be observed that the charge carrier channel's thickness remains consistent throughout the source and drain electrodes. Under this particular regime, the drain current exhibits a linear relationship with respect to the drain voltage. When the disparity between the gate voltage (V_{GS}) and the threshold voltage (V_{th}) is equivalent to the drain voltage (V_{DS}), as seen in **Figure 1.11(b),** the gate voltage is effectively reduced to zero at the drain electrode. As a result, the interface between the semiconductor and the insulator does not contain any charges at this moment. The channel has undergone a pinching-off phenomenon, resulting in the drain current reaching a saturation point where additional increases in the drain voltage no longer lead to a rise in current. When the voltage (V_{DS}) exceeds the difference between the gate voltage (V_{GS}) and the threshold voltage (V_{th}), the pinch-off occurs between the source and drain electrodes, as seen in **Figure 1.11(c).** The transistor operates in the saturation region, whereby the drain current ideally remains constant despite subsequent increases in the drain-source voltage (V_{DS}).

The drain current (I_{DS}) of a TFT in the linear regime can be given by-

$$I_{DS} = \frac{W}{L} C_{ox} \mu \left(V_{GS} - V_{TH} - \frac{V_{DS}}{2}\right) V_{DS};\ |V_{DS}| < |V_{GS} - V_{TH}| \tag{1.1}$$

The drain current in the saturation regime can be given by-

$$I_{DS} = \frac{W}{2L} \mu\, C_{ox} (V_{GS} - V_{TH})^2;\quad |V_{DS}| > |V_{GS} - V_{TH}| \tag{1.2}$$

In the given context, the variables W, L, C_{ox}, and μ represent the channel width, channel length, capacitance of the dielectric layer, and semiconductor mobility, respectively. When the value of V_{DS} is low, the squared term can be considered insignificant, resulting in a linear relationship between the drain current and V_{DS}. In the saturation regime, the current is equivalent to the value it attains at the pinch-off point. In the present scenario, the variable V_{DS} may be expressed as the difference between V_{GS} and V_{th}.

It is evident that the drain current remains unaffected by the variation in the drain-to-source voltage (V_{DS}). The saturation mobility, denoted as μ_{sat}, may be obtained by analyzing the gradient of a graph depicting the square root of the saturation drain current $(I_{DS})^{1/2}$ as a function of the gate voltage, V_{GS}. Similarly, the threshold voltage can be readily derived by calculating the point at which the graph intersects the current axis. The saturation regime is a regularly utilized context for reporting transistor properties [50].

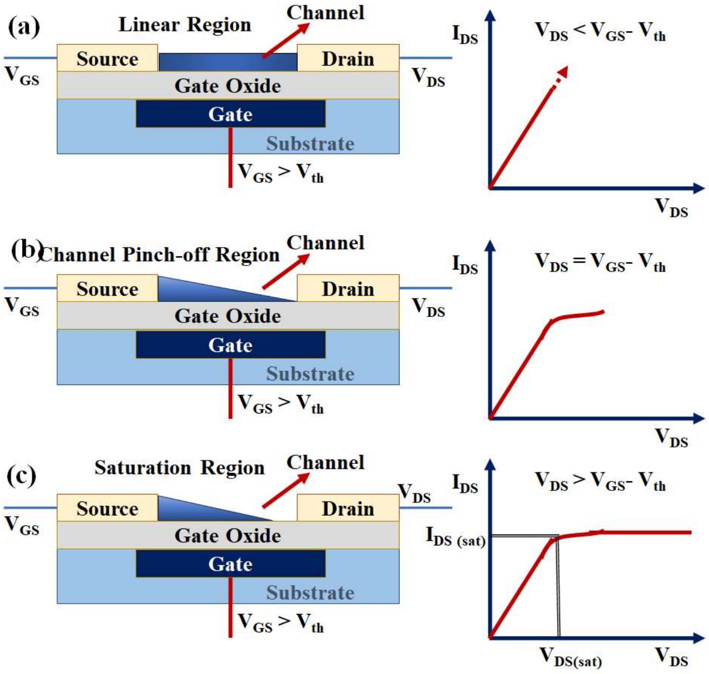

Figure 1.11 I_{DS} -V_{DS} (Drain characteristics) of n-channel TFT (a) Linear Region (b) Channel pinch-off region (c) Saturation region.

The above equations show that TFT works as a voltage-controlled current source. The vice-versa mechanism has been followed in the case of p-channel organic TFTs.

1.6.4. The characteristic curves of a transistor: output and transfer

The output curves depicted in **Figure 1.12** were generated by maintaining a constant V_{GS} value and thereafter altering V_{DS} throughout the range of 0 to -40 V. The transfer characteristics depicted in **Figure 1.12(b)** were obtained by establishing a fixed value for V_{DS} and thereafter varying V_{GS} throughout a broad spectrum of voltage values. The output curves exhibit a clear demonstration of the validity of **equation (1.1)** when the drain voltages are significantly smaller than the gate voltage. Specifically, it can be shown that the drain current (I_{DS}) exhibits a linear relationship with the drain voltage (V_{DS}). When the voltage is increased to greater levels, the quadratic component becomes more pronounced, resulting in an enhanced curvature in the figure. The occurrence of a saturation area, characterized by a constant drain current (I_{DS}), is observed when the voltage applied to the drain (V_{DS}) is almost equal to the voltage applied to the gate (V_{GS}), as stated by **equation (1.2).**

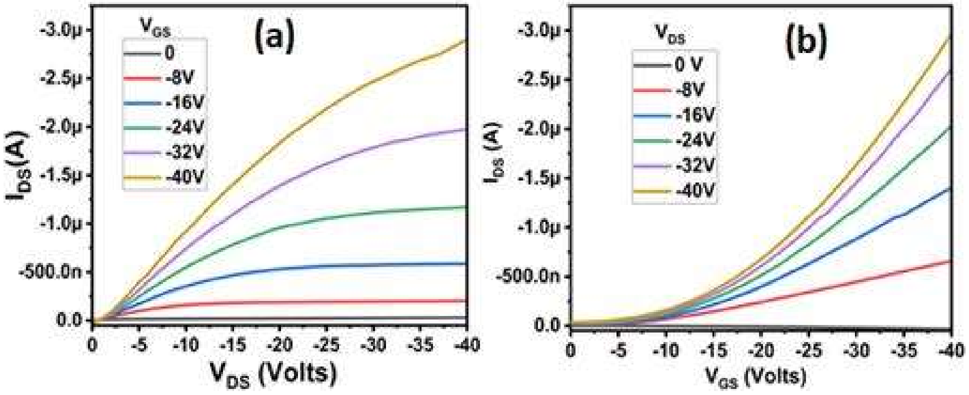

Figure 1.12 (a) Output characteristics and (b) Transfer characteristics of a typical TFT

The transfer curves demonstrate a linear relationship between the drain current (I_{DS}) and the gate-to-source voltage (V_{GS}) under the condition that V_{GS} minus the threshold voltage (V_{th}) is significantly greater than the drain-to-source voltage (V_{DS}). In the saturation regime, when the magnitudes of these voltages are similar, the drain current (I_{DS}) exhibits a quadratic relationship with respect to the gate voltage [50].

1.6.5. Transistors Parameters

Each device possesses its own set of standards, which also holds true for transistors. This section will focus on the examination of many essential metrics utilized for evaluating device performance, including charge mobility (µ), threshold voltage (V_{th}), subthreshold swing, and transconductance. In most cases, these parameters may be effectively represented by a transfer curve (I_{DS}–V_{GS}) and an output curve (I_{DS}–V_{DS}). **Figure 1.12** displays illustrations of both forms of curves.

Threshold Voltage: The threshold voltage refers to the minimal gate voltage necessary to accumulate charge carriers at the interface between the OSC (organic semiconductor) and insulator, hence establishing a conductive pathway between the source and drain. Typically, there is an objective for the threshold voltage to be minimized in order to enable the activation of a transistor with a relatively low voltage input. The investigation of the idea of threshold has been conducted by the research group led by Gilles Horowitz. The threshold voltage is often determined by analyzing a transfer curve within the framework of the proposed idea. Its value may be acquired by drawing a tangent line originating from the linear area of $(I_{DS})^{1/2}$ and extending it to intersect with the V_{GS} value on the abscissa [50].

Subthreshold Swing: The parameter known as 'subthreshold swing' has significance as it influences the rate at which the transistor transitions from an on state to an off state. The equation may be expressed as follows:

$$SS = \frac{dV_{Gs}}{d(log(I_{Ds}))} \tag{1.3}$$

The unit of S is expressed as millivolts per decade. A lower value of S signifies a reduced voltage change required, resulting in a faster transition of the device from the "on" state to the "off" state [50].

Charge Carrier Mobility: The field-effect mobility μ can be determined by analyzing the slope of the I_{DS} vs. V_{GS} curve in the linear regime and the $(I_{DS})^{1/2}$ vs V_{GS} curve in the saturation regime, as indicated by equations 1.1 and 1.2 [50].

Transconductance: Equations 1.1 and 1.2 show that the applied gate-source voltage in Organic Field Effect Transistors regulates the drain current. This is expressed quantitatively by the transconductance:

$$g_m = \frac{dI_{DS}}{dV_{GS}} \tag{1.4}$$

The assessment of the transconductance of a device is based on the transfer characteristics at a constant V_{DS}. When the negative gate-source voltage V_{GS} is increased, the drain current I_{DS} rises, which indicates the presence of a hole-transporting organic layer. The drain current of an electron-transporting material increases in response to an applied positive gate-source voltage [50].

1.7 Parameters of thin film affecting sensitivity

Thin films utilized to enhance the sensing response to hydrogen sulfide often exhibit distinct characteristics and features that enable them to be well-suited for sensing applications. The characteristics of the thin film are of utmost importance in achieving optimal performance in devices and sensing applications. The performance of thin films in gas sensing applications may be improved by optimizing parameters such as surface morphology, film thickness, and choice of sensing materials [21]. The following are a few notable characteristics which can be attributed to the enhanced sensing performance of any fabricated sensor.

Surface Morphology

Surface area: Thin films should have a significant surface area-to-volume ratio. This allows gas molecules to interact with the film, increasing gas adsorption and detection and sensor response.

Porosity: Thin films can be deliberately developed to possess a porous structure characterized by interconnecting spaces or pores. This facilitates the process of gas diffusion and encourages the interaction between gas molecules and the film, resulting in enhanced sensing capabilities.

Film Thickness

The thin film's optimal thickness should be determined to enhance the sensing response. The ideal thickness should establish a balance between facilitating fast gas diffusion and interaction with the active material while ensuring enough coverage and sensitivity.

Sensing Material

The thin film is typically composed of a sensing material that undergoes a measurable change in its electrical, optical, or physical properties upon exposure to the target gas. This material may be a metal oxide, a conducting polymer, or a composite material designed to exhibit a high sensitivity and selectivity towards the target analyte.

1.8 Motivation of the Thesis for Hydrogen Sulfide Sensors

Over the last several decades, there has been a rising demand for the development of an advanced gas sensor that exhibits superior performance and exceptional sensing properties. This sort of sensor is intended to be utilized in many fields, including industries, medical applications, and air quality management, among others. Hydrogen sulfide has been found to possess a high level of reactivity, toxicity, and a strong unpleasant odor [24]. This gas has the potential to impact the environment and poses a significant hazard to both living and non-living entities. Typically, prolonged exposure to hydrogen sulfide at a low concentration, measured in parts per million (ppm), might result in permanent visual impairment, throat infection, severe ailments, retinal irritation, and various respiratory disorders [25]. The release of hydrogen sulfide has adverse effects on both human and animal health, as well as on natural ecosystems. Excessive emissions have the potential to induce eutrophication and acidification in aquatic ecosystems, resulting in detrimental consequences such as reduced levels of biological oxygen demand (BOD) and alterations in species composition. Nowadays, hydrogen sulfide is regarded as one of the extensively processed hazardous inorganic compounds, originating from both natural and anthropogenic sources. Several manmade sources of environmental pollution include the breakdown process of manure, agricultural activities, and fertilizer enterprises [25]. A recent estimation indicates that the predominant source of hydrogen sulfide gas emissions is derived exclusively from the accumulation of animal manure and agricultural operations. The remaining hydrogen sulfide gas is generated by many industrial sectors, including the pharmaceutical industry. Ideally, it is desirable to maintain the concentration of this harmful analyte under a certain limit, expressed in parts per billion (ppb), in order to provide an optimal atmospheric environment. According to the guidelines set out by the Occupational Safety and Health Administration (OSHA), the acceptable threshold for this particular gas in the surrounding environment is a maximum of 15 parts per million (ppm) for a duration of 10 minutes and a maximum of 10 ppm for a period of 8 hours [25]. Hydrogen sulfide can emerge as a significant atmospheric pollutant owing to its corrosive, poisonous, and combustible properties. The precise monitoring of hydrogen sulfide in the environment is necessary in order to prevent catastrophic accidents and mitigate the risk of life-threatening diseases resulting from excessive exposure to hydrogen sulfide gas.

This thesis aims to comprehensively examine the fabrication and investigation of organic field effect transistors for the purpose of detecting hydrogen sulfide, with the ultimate goal of mitigating the occurrence of fatal accidents and casualties at diverse emission locations. The thesis also encompasses a novel improvement in the device fabrication procedure aimed at producing hydrogen sulfide sensors with low voltage requirements, cost-effectiveness, and low power consumption. Furthermore, the thesis chapters provide a comprehensive analysis of the sensing outcomes and sensing process associated with organic thin-film transistors (OTFTs) based on conductive polymer/conductive polymer nanocomposites, specifically for the detection of hydrogen sulfide (H_2S) under ambient conditions.

In conclusion, a comprehensive understanding of the properties, sources, health hazards, and regulatory standards related to hydrogen sulfide is essential for developing effective gas-sensing technologies. The fabrication and characterization of organic thin film transistors for H_2S gas sensing applications contribute significantly to mitigating the risks associated with this toxic gas in various industrial and environmental settings.

1.9 Literature Review and Problem Statement

Table 1.4, presented below, elaborates on the literature survey of the works related to hydrogen sulfide gas detection. Various types of materials and thin film deposition methods have been utilized for efficient hydrogen sulfide detection. Metal oxide semiconducting (MOS) materials are a more explored class of materials in this regard. MOS-based sensors suffer from limited selectivity, higher temperature requirements for operation, and complex deposition methods. Moreover, most of the hydrogen sulfide gas sensors suffer from prolonged recovery time, possibly due to the gas's highly corrosive and reductive nature.

This thesis aims to fabricate highly efficient hydrogen sulfide gas sensors with a facile low-cost deposition method, high sensor response at lower concentrations/ sub-ppm regime, fast response/ recovery characteristics, excellent selectivity and repeatability, and room temperature operability.

Table 1.4 Literature Review of Hydrogen Sulfide Gas Sensors

Sensing material	**Deposition Technique**	**Temp.**	**Sensitivity (ppm)**	**Response/Recovery time**	**Remarks (Ref.)**
CuO/MoS_2	Layer-by-layer self-assembly	RT	61% (30 ppm)	26/18 sec	High response time and poor sensor response at lower concentrations [51]
D2-Hept-BTBT-Hex/ Cu-TPP	Langmuir-Schaeffer	RT	~50% (5 ppm)	40sec/ 60 min	Poor response-recovery characteristics and poor sensor response at lower concentrations [13]
P3HT/GQD	Floating film transfer method (FTM)	RT	~33% (5 ppm)	10/225 sec	Poor sensing response at lower concentrations, higher LOD, and response time [52]
$MoSe_2$ nanoflakes	Liquid phase exfoliation	200 °C	53% (5.45 ppm)	15/43 sec	High temperature of operation, poor sensor response at lower concentrations [53]
g-C_3N_4/α -Fe_2O_3	Screen printing	RT	55% (10 ppm)	52.5/8 sec	High response time and poor sensor response at lower concentration, higher LOD [54]
SnO_2/rGO	Hydrothermal	125 °C	34.3% (100 ppm)	209/900 sec	Higher operating temperature, poor sensitivity, and poor response/recovery behavior [55]
PPy/WO_3	In-situ photopolymerization	RT	81% (1 ppm)	6/210 min	Higher LOD and prolonged recovery behavior [56]
Al doped ZnO	Spray pyrolysis	200 °C	63.8% (150 ppm)	90/209 sec	Higher operational temperature and poor sensor response and response-recovery kinetics [57]
rGO loaded/CuO nanofiber	Electrospinning	300 °C	91.5% (10 ppm)	~350/300 sec	High operation temperature, poor response-recovery time [58]

$CuO/CuFe_2O_4$	Simple heating route using water bath and facile two step method	240 °C	95.5% (10 ppm)	31/40 sec	Higher operational temperature and poor response time [59]
porous SnO_2-CuO nanotubes	Electrospinning	200 °C	99.9% (5 ppm)	5.27 sec/ 36 min	Higher operating temperature, prolonged recovery time [60]

1.10 Resources utilized in Device fabrication and Sensing characterization

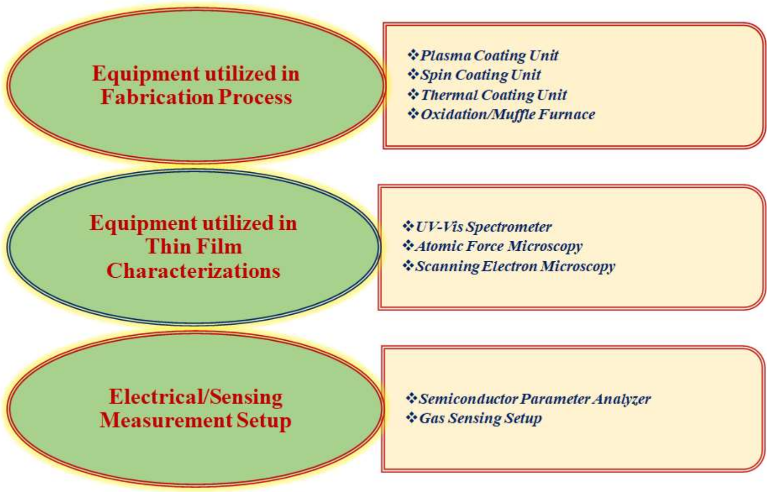

Figure 1.13 Resources utilized in OTFT fabrication and characterization.

The equipment/tools in the device fabrication process, film characterization process, and electrical/sensing measurement setup are illustrated in **Figure 1.13**.

1.11 Outlines of the Thesis

The thesis is structured into five chapters in order to comprehensively explore all aspects of fabrication and film/sensing characterization during my doctoral degree. The thesis encompasses many key components, including an introductory section, an exploration of the underlying mechanism of organic semiconductors, an examination of the functioning of thin-film transistor (TFT) devices, an analysis of the fabrication facilities employed in the production of organic thin-film transistors (OTFTs), and a study of the OTFTs created specifically for the purpose of hydrogen sulfide sensing application. The organization of the thesis chapters is as follows-

Chapter 1. The introduction of various topics, including the thesis abstract and the evolution of TFTs, is explained in this chapter. The topics covered are as follows.

- *Thesis Abstract*
- *Introduction on TFTs*
    - *Organic Semiconductors and their Deposition Methods*
    - *Gate Dielectrics and their Deposition Method and Complexities*
- *Schematic and Charge Transport Mechanism in TFTs*
- *Broad Area Application of OTFTs*
- *Resources utilized in OTFT Fabrication and Characterization*
- *Outlines of the Thesis*

Chapter 2: This study investigates the significance of organic polymers in the production of organic thin-film transistors (TFTs), specifically focusing on their distinct characteristics in hydrogen sulfide sensing applications. This chapter has examined an organic polymer PCPDTBT-based organic thin-film transistor (OTFT) with the subsequent research highlights.

- *Device Fabrication Steps*
- *Thin Film Characterization*
- *Electrical and Sensing Parameters*
- *Device Results and Sensing Mechanism*
- *Conclusion*

Chapter 3: This chapter presents an investigation of a solution-processed organic thin-film transistor (OTFT) composed of an organic polymer composite PCPDTBT/CdS. The primary focus of this research is to explore the potential of this composite for hydrogen sulfide sensing applications. The key research highlights are as follows.

- *Device Fabrication Steps*
- *Thin Film Characterization*
- *Electrical and Sensing Parameters*
- *Device Results and Sensing Mechanism*
- *Conclusion*

Chapter 4: This study investigates the fabrication and characterization of a hybrid inorganic high-k dielectric-based organic thin film transistor designed for the purpose of hydrogen sulfide detection. The chapter encompasses a comprehensive integration of high-k dielectric-based gate oxide and polymer/2D nanocomposite-based organic semi-conductor channel, with the aim of enhancing the hydrogen sulfide sensing capability. The chapter presents the key study findings in a concise manner.

- *Device Fabrication Steps*
- *Thin Film Characterization*
- *Electrical and Sensing Parameters*
- *Device Results and Sensing Mechanism*
- *Conclusion*

Chapter 5: concludes the summary and future scope of the research work presented in the previous chapters.